Magnetic Mirror Structures Observed by Cluster in the Magnetosheath

O. D. Constantinescu[1,2], K-H. Glassmeier[1,3], R. Treumann[4], K-H. Fornaçon[1]

Abstract.

We present a method for identification of magnetic mirror structures (MMS) in multi-point spacecraft measurements and for deriving their full 3D geometry. Multiple minima in magnetic field data are no longer regarded as separate MMS but as belonging to the same mirror structure. The approach is based on fitting a model magnetic field to measured data from one or many spacecraft. Because of the complexity of the model magnetic field, fitting the data from only one spacecraft has proved not to be reliable even if data from the others spacecraft can be used for checking the results. The main reason is the instability of the numerical fit and the non-uniqueness of the solution found. However, performing the fit on the data from multiple spacecraft allow the use of information from different regions of the structure eliminating false results and improving the numerical stability of the fit.

1. Introduction

Magnetic mirror structures [*Hasegawa*, 1969; *Southwood and Kivelson*, 1993] are common in anisotropic space plasmas. They can often be found in the terrestrial magnetosheath [*Crooker and Siscoe*, 1977; *Tsurutani et al.*, 1982]. Because of their potential to infer about the magnetic topology at points separated by distances of the order of the magnetic mirror dimensions, the four Cluster spacecraft constitute an adequate tool for studying the geometrical structure of magnetic mirrors.

We use the same data interval on which *Lucek et al.*, [2001] already identified strong mirror activity (10 Nov 2000 (Day 315) 08:20 - 08:25 UT). When these measurements took place the Cluster constellation was situated in the dusk side magnetosheath. The spacecraft separation was about 1000 km with GSE velocities about 1 km/s. By correlation analysis corroborated with Wind observations *Lucek et al.*, [2001] came to the conclusion that the plasma flow velocity was of 815 km/s in the direction C1 - C3. (We refer to Cluster spacecraft number n as "Cn")

[1]Institut für Geophysik und Meteorologie, Mendelssohnstrasse 3 38106 Braunschweig Germany

[2]Institute for Space Sciences, Atomistilor 111, P.O. Box MG-23, R-76911 Bucharest Romania

[3]Max-Planck Institut für Aeronomie, Lindau, Germany

[4]Max-Planck Institut für extraterrestrische Physik, Garching, Germany

Paper number .
0094-8276/03/$5.00

2. Magnetic Mirror Model

The magnetohydrostatic model for magnetic mirror (MMS) is based on the following assumptions [*Constantinescu*, 2002]: the distribution function of the plasma is bi-Maxwellian, the unperturbed magnetic field is uniform, the perturbation is small compared with the average magnetic field, the perturbation is symmetric around an axis parallel to the unperturbed magnetic field, the perturbation is periodical along the symmetry axis, and the field-aligned currents are negligible.

These assumptions are not fully satisfied inside magnetosheath but we can safely assume there are regions with relatively uniform magnetic field where MMS will develop after the solar wind has passed through the shock . The symmetry of MMS probably will break when they approach the magnetopause. The quasiperiodic character of observed MMS justifies the periodicity assumption

Under these assumptions the MMS model predicts a magnetic field perturbation of the form [*Constantinescu*, 2002]:

$$\delta B_\rho(\rho,z) = \frac{2\pi}{\alpha}\sum_{n=1}^{\infty} J_1\left(\frac{n\alpha\rho}{L}\right) \left[a_n \sin\left(\frac{n\pi z}{L}\right) - b_n \cos\left(\frac{n\pi z}{L}\right)\right] \quad (1)$$

$$\delta B_z(\rho,z) = 2\sum_{n=1}^{\infty} J_0\left(\frac{n\alpha\rho}{L}\right) \left[a_n \cos\left(\frac{n\pi z}{L}\right) + b_n \sin\left(\frac{n\pi z}{L}\right)\right] \quad (2)$$

where (ρ,φ,z) are the radial distance, azimuth angle and height in cylindrical coordinates, $2L$ is the period of the perturbation along the average magnetic field, J_k is the k-order cylindrical Bessel function, and

$$\alpha = \pi\sqrt{\frac{\frac{1}{2}\left(1-\frac{1}{A_0}\right)+\frac{1}{\beta_{0\perp}}}{A_0-1-\frac{1}{\beta_{0\perp}}}} \quad (3)$$

$A_0 = T_\perp/T_\parallel$ being the anisotropy (ratio between orthogonal and parallel temperature) , $\beta_{0\perp}$ the plasma parameter, i.e. the ratio between the orthogonal plasma pressure $p_{0\perp}$ and the magnetic pressure $B_0^2/2\mu_0$ and a_n and b_n are constant Fourier coefficients.

Equations (1,2) describe a magnetic field with complex geometry even if we take into account only the first Fourier order (Figure 2). For the first Fourier order we can imagine the MMS consisting of coaxial layers wrapping around each other. Each such layer corresponds to a given sign of the first order Bessel function in the expression of the radial component of the perturbation (1). The surfaces between these layers correspond to the zeroes of the Bessel function. They form coaxial cylinders with straight magnetic field lines. The central structure represents the classical image of a magnetic

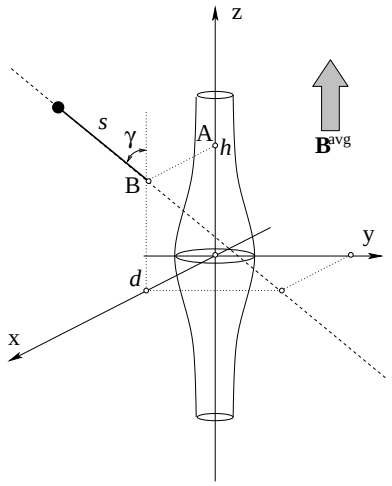

Figure 1. *The normal coordinates. The dashed line is the spacecraft path which intersects the (x-z)-plane of the MMS system in the point B(d,0,h) and is parallel with the (y,z)-plane. The angle between the trajectory and the z-axis is γ and the distance between the spacecraft and the point B is s.*

bottle. The model provides no information about the size of MMS. However, it provides a relation between the radius and the length of the central structure:

$$\alpha R/L = 3.832 \tag{4}$$

This also expresses approximatively the thickness of the layer. For typical magnetosheath conditions L/R ratio varies between 1 and 3 (Figure 3)

3. Fitting Procedure

Because of the large number of free parameters in the expressions (1) and (2), the fit is sensitive to the choice of start parameters. Therefore we must determine the level of confidence of the results by analyzing the stability of the fit with respect to changes of the start parameters and variations in the measured data.

Thanks to the symmetry properties of the MMS we can choose a MMS coordinate system which has the (y, z)-plane parallel to the spacecraft trajectory. The position of the spacecraft trajectory relative to the MMS is defined by three parameters (Figure 1): the angle $\gamma \in [0, \pi/2]$ between spacecraft path and the axis of the MMS, the distance $d \in [0, \infty)$ between spacecraft path and the MMS axis and the distance $h \in (-L, L]$ between the center of the MMS and point A in Figure 1.

Knowing the trajectory coordinates, the position of the spacecraft relative to the MMS can be specified by one additional coordinate: $s \in (-\infty, +\infty)$, the distance between the point B in Figure 1 and the spacecraft. We will name (h, d, γ, s) *normal coordinates*. The usual cylindrical coordinates can be expressed in terms of normal coordinates.

The dimension of the fitting window is 200 data points, corresponding to about 9 seconds or 7000 km. (we use a resolution of 22 vectors per second) Depending on the values of L and α (4) this corresponds to several layers of the MMS. For $L = 5000$ km the spacecraft will pass through 1-2 layers for $\alpha = 5$, and through 3-4 layers for $\alpha = 10$.

The parameters used for the fitting are: trajectory normal coordinates (h, d, γ), initial position of the spacecraft on its path (s_0), the length of the MMS (L), the unperturbed magnetic field intensity (B_0), α, and the Fourier coefficients a_j and b_j. We go up to $n = 4$ in the Fourier expansion, as adding higher orders only reproduces the "small scale" structures not relevant for our study.

The fit for one spacecraft produces a set of parameters for the data subinterval $[i, i + 200]$. If the minimization con-

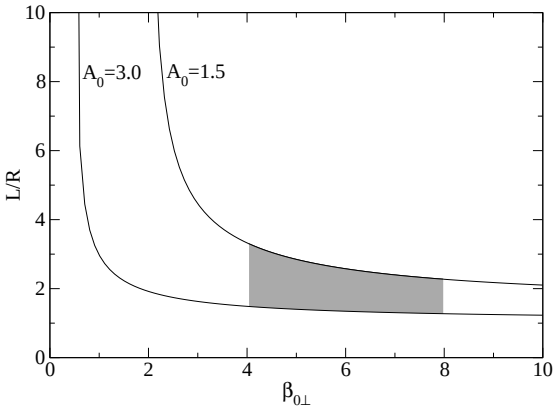

Figure 3. *Dependence of L/R ratio on plasma parameters. The gray area represents typical magnetosheath conditions. It can be seen that MMS are more elongated for low anisotropy and low β (close to the instability condition) but less elongated (spheres) for high anisotropy and high β.*

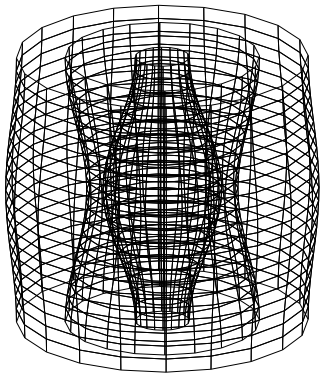

Figure 2. *The surfaces defined by the field lines for the first Fourier component of the magnetic field perturbation. [Reprinted from JASTP, Vol 64, D. Constantinescu, Self-consistent model of mirror structures, 645-649, Copyright (2002), with permission from Elsevier]*

Table 1. *Normal coordinates and model parameters*

d^{ref}	=	1490 km	a_1	=	4.5	b_1	=	16.7
h^{ref}	=	383 km	a_2	=	11.3	b_2	=	33.3
γ	=	73.9^o	a_3	=	-24.8	b_3	=	-0.7
L	=	6186 km	a_4	=	-19.8	b_4	=	-13.4
B_0	=	52.2 nT						
α	=	11.5						

verges and the parameters have reasonable (physical) values, they are used as start parameters for the next data subinterval $[i+n, i+n+200]$. Otherwise the default values will be used. We usually take $n = 2$ (99% overlapping intervals).

After scanning the whole data interval we will have about 3000 sets of parameters (one set for each subinterval). These can be inspected representing the parameters versus the number (i) of the data subintervals which have produced them.

For a successful scan we expect to see the parameters grouped close to each other for each region where a MMS was present in the data. All parameters but s should be grouped around constant values corresponding to their average values, so the shapes of their groups should suggest horizontal lines. The s groups should reflect the motion of the spacecraft on its path. The s groups should also be linear but with the same positive slope. These characteristics have been observed though, due to the large number of free parameters involved in the minimization, we cannot have complete confidence in these results. One way to check the quality of the fit is to use the resulting parameters to calculate the magnetic field predicted by the model at the locations of the other three spacecraft and compare the result with the data.

4. Multi-spacecraft fit

Having found a MMS by fitting the data from one spacecraft, we can calculate the normal coordinates for the other (witness) spacecraft and propagate the model magnetic field to their locations. By comparing the predicted magnetic field with the magnetic field measured by the witness spacecraft, the quality of the fit can be tested.

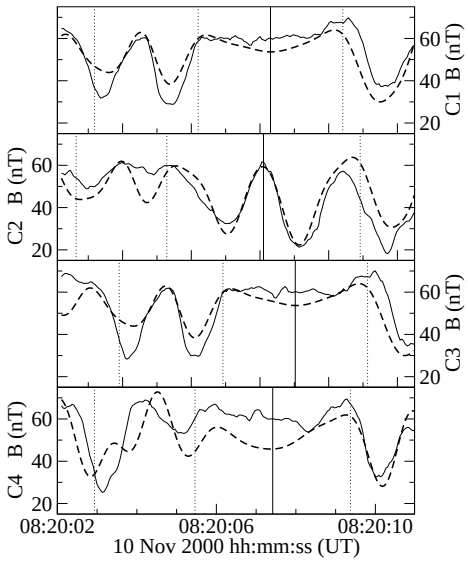

Figure 4. *Measured (solid lines) and model (dashed lines) magnetic field intensity for the four Cluster spacecraft. C1 and C2 were participating in the fit, C3 and C4 were witness spacecraft. The vertical solid lines represent the intersection with (x, z) plane (i.e. $s = 0$) and the vertical dotted lines separates different layers of the MMS*

We can use the technique described in section 3 for each of the four Cluster spacecraft. In addition we introduce a model propagation after each successful fit and we compute the correlations between the field that result from the propagation and the measured magnetic field.

Even if we gain more confidence in the fit results by comparing the propagated magnetic field with the measured data, the numerical code is still unstable to small changes in the initial parameters. This is due to the large number of parameters involved. However, this method helps us to select those regions where the probability of MMS presence is high and provides some parameters which can be used for further investigation.

One step further is to simultaneously fit data from $1 < n \leq 4$ spacecraft making use of the normal coordinates introduced in section 3. For one of the n satellites which participate in the fit, designated as the "reference spacecraft" we choose some starting guess parameters and calculate the starting normal coordinates for the other $n-1$ spacecraft. Knowing the normal coordinates we simultaneously fit the

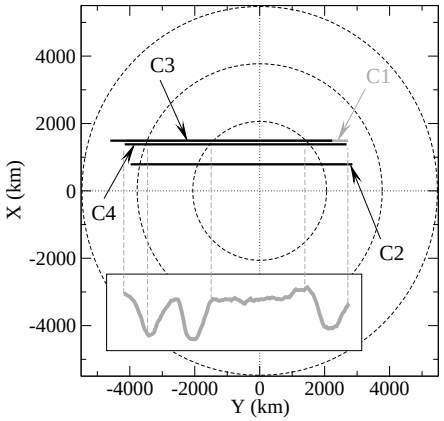

Figure 5. *The projections of the spacecraft trajectories in the (x-y) plane(straight lines) and the magnetic field measured by C1 (gray curve). The circles represent the boundaries between different layers.*

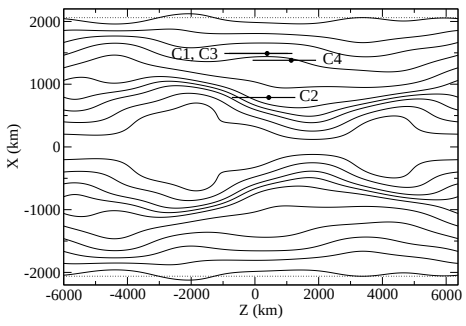

Figure 6. *The magnetic field lines derived from the model. The straight lines are the projections of the spacecraft trajectories on the (x-z) plane. The dots are the points where the spacecraft paths intersect the (x-z) plane.*

data from the n selected spacecraft. With the resulting parameters we calculate the model magnetic field for the remaining $4-n$ spacecraft and determine the correlations between the measured magnetic field and the fit/(propagation) model magnetic field.

A procedure similar to the one described in section 3 can be implemented for scanning the magnetic field data in the case of multi-spacecraft fitting, additional information being provided by the correlations between model and measured magnetic fields for the witness spacecraft.

5. Case study

As for an example we selected one event which occurred in the time interval [08:20:00, 08:20:10] UT. This is a rather exceptional case where the agreement between the model and the witness spacecraft is very good. C1 and C2 were chosen to participate in the fit, C1 being the reference spacecraft. C3 and C4 are the witness spacecraft. The reason of our choice is the large separation between C1 and C2 in the direction orthogonal to the average magnetic field. Because of this, C1 and C2 sample different layers of MMS encountered. Due to the fact that the plasma was flowing in the direction C1 - C3 [*Lucek et al.* 2001] the magnetic field measured by C3 is very similar to the magnetic field measured by C1. As a consequence the comparison for C3 is irrelevant. The resulted correlations are: $C_1 = 0.81$, $C_2 = 0.83$, $C_3 = 0.78$, $C_4 = 0.64$. The parameters obtained from the fit are given in Table 1.

By making use of expression (4) the radius of the main structure is obtained as: $R = 2061$ km.

In Figure 4 we plot the measured magnetic field intensity against the magnetic field intensity derived from the model. The vertical continuous lines mark the intersection with the (x, z) plane, i.e. the time when the distance (d) between spacecraft and the axis of the MMS was minimum. The vertical dotted lines mark the boundaries between different layers. We note that the multiple minima in Figure 4 are the result of passing through different regions of the same magnetic mirror structure. From Figure 5 we can see the way the spacecraft pass through the layers of the structure identified. Here the boundaries are represented by dashed circles.

The magnetic field lines in the $(x - z)$ plane that are reconstructed from the model, as well as the projections of spacecraft trajectories on this plane are shown in Figure 6. This figure reveals that C1, C3 and C4 are passing through a region of the central structure where the magnetic field is almost uniform. This corresponds to the plateaus in Figure 4. C2 flew much closer to the axis of the MMS and measured violent changes in the magnetic field inside the central structure.

In the general case after a MMS has been found using $n < 4$ spacecraft, it is possible to improve the quality of the parameters by performing a new fit using all four spacecraft and the previous parameters as start parameters. For this particular event the new parameters are very close to the old ones.

6. Conclusions

We analyzed different methods that could be used for identification of MMS in spacecraft data based on the geometry of the magnetic field. The simplest approach is to fit the model magnetic field to the data measured by a single spacecraft. Even if a scanning procedure which enables us to find regions where the probability of existence of MMS is high was developed, the numerical code is unstable with respect to changes of the start parameters. By calculating the magnetic field predicted by the model at the locations of the other spacecraft and comparing it with the measured data we can gain a certain degree of confidence. However by simultaneously fitting the data from multiple spacecraft we achieve satisfactory stability with respect to changes of the start parameters. Future work will include fitting each component of the magnetic field. A statistical study will be carried out in order to validate these preliminary results. We also should keep in mind the assumptions on which the model used is based (Section 2). In particular the assumption of small perturbations is not always satisfied, this resulting in unreasonably large perturbations of the predicted magnetic field near the symmetry axis. If the other assumptions (symmetry, periodicity, uniform magnetic field) are not satisfied either the fit procedure will not converge or the observations from the witness spacecraft will not agree with the model field. For the studied 5 minutes interval this is usually the case, the presented case study being the best example of successful identification.

Adding C4 to the fit leads to similar results for the event presented but if we change the pair of spacecraft which participate in the fit the convergence is lost. For all other but (C2,C4) pairs this can be explain by too small separation in the direction orthogonal to the average magnetic field

By applying multi-spacecraft fit method to one MMS structure we here demonstrate the power of the method which allowed us to derive the detailed structure of MMS. This method also provides a way to derive the parameter α, which is related to the plasma, solely based on magnetic field measurements.

Acknowledgments. This work was financially supported by the German Bundesministerium für Bildung und Forschung and the Deutsches Zentrum für Luft und Raumfahrt under contract `50OC0103`.

References

Crooker, N.U. and G.L. Siscoe, A mechanism for pressure anisotropy and mirror instability in the dayside magnetosheath, *J. Geophys. Res.*, 82, 185, 1977

Constantinescu, O.D., Self-consistent model for mirror structures, *Journal of Atmospheric and Terrestrial Physics*, 64, 645-649 2002

Hasegawa, A., Drift mirror instability in the magnetosphere, *Phys. Fluids*, 12, 2642, 1969

Lucek, E.A., M.W. Dunlop, T.S. Horbury, A. Balogh, P. Brown, P. Cargill, C. Carr, K.-H. Fornacon, E. Georgescu and T. Oddy: Cluster magnetic field observations in the magnetosheath: four-point measurements of mirror structures, *Annales Geophysicae*, 19, 1421-1428, 2001

Southwood, D.J. and M.G. Kivelson, Mirror instability: 1. Physical Mechanism of Linear Instability, *J. Geophys. Res.*, 98, 9181, 1993

Tsurutani, B.T., E.J. Smith, R.R. Anderson, K.W. Oglivie, J.D. Scudder, D.N. Baker and J.S. Bame, Lion Roars and nonoscilatory drift mirror waves in the magnetosheath, *J. Geophys. Res.*, 87, 6060, 1982

O. D. Constantinescu, Institut für Geophysik und Meteorologie Technische Universität Braunschweig Mendelssohnstrasse 3 38106 Braunschweig Germany (d.constantinescu@tu-bs.de)

(Received _____.)